

# Impurity compression and enrichment studies on Alcator C-Mod

J.A. Goetz, B. Lipschultz, C.S. Pitcher, J.L. Terry, P.T. Bonoli, J.E. Rice, and S.J. Wukitch

*MIT Plasma Science & Fusion Center, Cambridge, MA 02139, USA*

## Abstract

Impurity transport has been investigated in the reactor-like conditions of the Alcator C-Mod divertor (divertor plasma density  $\geq 10^{21} \text{ m}^{-3}$ , parallel heat flux in the SOL  $\leq 0.5 \text{ GW-m}^{-2}$ ). Trace amounts of the recycling impurity gases helium, neon, argon, and krypton were injected into plasmas. A residual gas analyzer that samples the private flux region of the divertor was used for divertor impurity neutral density measurements. Compression ratios ( $C_Z$ ) of up to 400 and enrichment factors ( $\eta_Z$ ) of up to 20 have been observed for argon in Alcator C-Mod discharges. Compression ratios increase and enrichment values are constant or slightly increasing with line-averaged density for argon in Ohmic discharges. Above the divertor detachment threshold density,  $C_Z$  and  $\eta_Z$  both decrease. During H-mode operation, compression and enrichment ratios for argon decrease relative to their Ohmic values. For similar plasma conditions, impurity compression ratios and enrichment values increase with the mass of the impurity. This mass scaling may be partially explained by the decrease in the ionization mean-free-path with increasing impurity mass.

## 1. Introduction

It is envisioned that dissipative divertor operation will be necessary for a fusion reactor to tolerate the power flowing to the divertor plates. Large volumetric losses are thus required in the divertor region to dissipate this power and reduce the heat loads on the divertor plates to technically feasible levels [1]. These scenarios will probably require the use of seeded impurities to radiate this power and will further emphasize the already important issues of impurity transport and exhaust. In order to minimize the detrimental effect of such impurities on the core plasma, including fuel dilution and cooling, impurities must be confined to the divertor with minimal concentrations in the core and scrape-off layer (SOL) plasma. This preferential compression of impurities would also aid in pumping helium born in the core plasma.

The retention of recycling impurities in a divertor is determined both by the distance a neutral impurity atom travels before it is ionized and the action of a variety of forces [2,3]. Two measures of this divertor retention are impurity compression and impurity enrichment. Impurity compression can be defined as:

$$C_Z = \frac{n_{0,Z}^{\text{div}}}{n_Z^{\text{core}}}, \quad (1)$$

where  $n_{0,Z}^{\text{div}}$  is the divertor impurity neutral density and  $n_Z^{\text{core}}$  is the core impurity ion density. Maximizing  $C_Z$  will result in more power exhaust through radiation in the divertor and in less contamination of the core plasma. Impurity enrichment can be defined as:

$$\eta_Z = \frac{C_Z}{C_D}, \quad (2)$$

where  $C_D = 2n_{D_2}^{\text{div}} / \bar{n}_e^{\text{core}}$  is the deuterium compression. Impurity particle exhaust is enhanced by enriching the impurity level with respect to the fuel gas in the divertor. This should aid in the removal of the impurity by pumping.

Experiments have been performed on Alcator C-Mod with the recycling impurities helium, neon, argon, and krypton to investigate these impurity transport issues. Similar experiments have also been done on the ASDEX-Upgrade [4], DIII-D [5], and TdeV [6] tokamaks with helium and neon gases.

## 2. Experiment description

Alcator C-Mod is a compact, high-field tokamak with a “vertical-plate” divertor geometry and molybdenum walls and divertor plates. See Ref. [7] for a general description of the tokamak and its principal diagnostics. It operates routinely in either the high-recycling or the detached divertor regime. To investigate impurity transport in the reactor-like conditions of the Alcator C-Mod divertor (divertor plasma density  $\geq 10^{21} \text{ m}^{-3}$ , parallel heat flux in the SOL  $\leq 0.5 \text{ GW-m}^{-2}$ ), trace amounts of the recycling impurity gases helium, neon, argon, and krypton were injected into plasmas of varying character; Ohmic, L-mode, H-mode, detached divertor, *etc.* The gases were puffed from either the outer midplane or the divertor slot with a piezoelectric valve, although for recycling gases, puff location is not an important factor in core penetration [8]. The core impurity ion density is measured with a variety of methods and the divertor impurity neutral density is measured with a quadrupole mass spectrometer [9,10]. This mass spectrometer, also known as a residual gas analyzer (RGA), samples the private flux region of the divertor. This technique is different than other measurements of impurity neutral density in the divertor which use modelling of the temporal behavior of the core impurity level [4,6] or the impurity emission from a Penning gauge [5].

The RGA is located some distance ( $\sim 1.7 \text{ m}$ ) from the divertor volume and is isolated from it by a pressure-limiting aperture. Figure 1 is a schematic that shows the location of the RGA volume with respect to the lower closed divertor. The aperture is used to limit the pressure in the RGA volume to less than 0.1 mTorr because the pressure in the vertical port can reach values greater than 150 mTorr. Therefore, measurements made in the RGA vacuum chamber must be transformed to reflect what is actually in the tokamak divertor volume.

This transformation is a two-step process. The first step involves solving an equation for molecular flow through an aperture between two chambers [11]. In this case the chambers

are the vertical port and the RGA volume. The partial pressure in the RGA volume,  $P_{\text{RGA}}$ , is related to the partial pressure at the bottom of the vertical port,  $P_{\text{port}}$  (Fig. 1), by:

$$P_{\text{port}} = \left(\frac{V}{C}\right) \frac{dP_{\text{RGA}}}{dt} + \left(\frac{S+C}{C}\right) P_{\text{RGA}}, \quad (3)$$

where  $V$  (RGA volume) = 1.2 liters,  $S$  (pumping speed) = 16 liter/s, and  $C$  (aperture conductance) =  $1.33 \times 10^{-2}$  liter/s (for  $D_2$ ). The second step involves a transform of  $P_{\text{port}}$  up the vertical port to obtain the partial pressure of the impurity in the divertor region,  $P_{\text{div}}$  (Fig.1):

$$P_{\text{div}} = P_{\text{port}} + \tau \frac{dP_{\text{port}}}{dt}, \quad (4)$$

where  $\tau$  = port delay time  $\sim 0.05$  s for  $D_2$ . The delay times and RGA vacuum chamber characteristics are determined from gas puff calibrations. Conductance and delay time scale with  $1 / \sqrt{\text{impurity mass}}$ .

An example of such a deconvolution for a calibration puff into an evacuated torus is shown in Fig. 2. The actual torus pressure measured with an ionization gauge is shown by the solid line. In this case the pressure in the torus is equivalent to the pressure in the divertor.  $P_{\text{RGA}}$  is shown by the dashed line and the deconvolved  $P_{\text{div}}$  by the squares. The agreement between the deconvolved  $P_{\text{div}}$  and the actual measured pressure in the torus is good. Obtained from such a gas puff is a current/pressure sensitivity factor for each impurity. Calibration puffs have been done over a range of deuterium pressures from 0 to 120 mTorr. This RGA has good sensitivity,  $\sim 3.5 \times 10^{-4}$  A/Torr for argon, and “fast” time response, typically 30 ms per acquired mass.

A variety of methods is used to determine the impurity density in the core plasma. The helium used is the  $^3\text{He}$  isotope because the  $^4\text{He}$  isotope cannot be distinguished from the deuterium fuel gas by the RGA. The power deposition profile due to mode conversion electron heating in  $\text{D}(^3\text{He})$  ICRF-heated discharges is used to determine the core helium density. The deposition profile is measured by modulating the ICRF power and then carrying out a break-in-slope analysis of the electron temperature temporal behavior. The core helium density is accurately inferred by varying the  $^3\text{He}$  concentration in a full-wave ICRF code [12] until the electron power deposition profile predicted by the code agrees with the measured profile.

Core neon and krypton emission lines are measured with an extreme-ultraviolet spectrograph [13]. Impurity ion charge-state densities are calculated using the MIST impurity transport code [14] with the appropriate transport coefficients [15]. In conjunction with an atomic physics package, the MIST calculated impurity density profiles are converted to impurity emission line-brightness and then scaled to match the measured line-brightness. The total impurity density is then obtained by summing the individual charge-state densities.

A similar technique is used to determine the core argon ion density. The emission lines from He-like argon are measured with an x-ray crystal spectrometer [16]. However, coronal equilibrium, *i.e.* no transport, is assumed to calculate the fully stripped, H-, He-, and Li-like argon density profiles. The rest of the argon density calculation follows as above. The

determination of the core argon ion density is the most accurate because the charge-state used to calculate the normalization factor is located in the center of the discharge. The charge-states used for the neon and krypton normalizations are located nearer the edge of the plasma and are thus more dependent on the transport coefficients used in the charge-state balance calculation and more dependent on the local density and temperature.

### 3. Results

Measurements of impurity compression,  $C_Z$ , and impurity enrichment,  $\eta_Z$ , have been made in a variety of discharges with puffed recycling gases. Figure 3 shows the time behavior of an Alcator C-Mod discharge for which impurity compression and enrichment measurements of argon were made. This was a 1.0 MA, lower single-null attached divertor discharge that had  $\sim 9 \times 10^{17}$  argon atoms puffed into it at 0.3 s, Fig. 3(b). The divertor argon neutral density,  $n_{0,Ar}^{div}$ , and the core argon density,  $n_{Ar}^{core}$ , are shown in Fig. 3(a) and (b), respectively. It is seen that the neutral argon builds up in the divertor and is fairly constant by 0.7 s. The core argon density level reaches a steady level somewhat earlier. This is typical of a recycling gas such as argon. Shown in Fig. 3(c) and (d) are the divertor neutral deuterium density,  $n_{0,D}^{div}$ , and the line-averaged core electron density,  $\overline{n_e^{core}}$ , which for the measured  $Z_{eff} \sim 1$  is equal to,  $\overline{n_D^{core}}$ . The argon compression,  $C_{Ar}$ , and enrichment,  $\eta_{Ar}$ , are shown in Fig. 3(e) and (f) respectively. The compression of argon increases as the divertor pressure increases, eventually reaching an equilibrium value of about 350 to 400 for this particular discharge. The enrichment of argon also increases during this time period, and reaches a steady value of approximately twenty.

Argon is usually puffed in trace amounts into Alcator C-Mod plasmas to facilitate ion temperature measurements. As a result, there is a wide range of discharges for which compression and enrichment values are measured. Figure 4 is a summary of these measurements. It is seen in Fig. 4(a) that the compression of argon increases, up to values of greater than 350, with increasing line-averaged density in attached Ohmic plasmas (open squares). Enrichment values are relatively constant or increase slightly as the density is raised below the detachment threshold, see Fig. 4(c). This implies that the argon compression is increasing with line-averaged density at least as fast as the deuterium compression, see Fig. 4(b). The dependence of  $C_{Ar}$  and  $\eta_{Ar}$  on the divertor neutral pressure is similar to that of line-averaged density. This is because of the relationship of divertor neutral pressure to the line-averaged density in Ohmic plasmas [17].

The scaling of impurity compression and enrichment change substantially at higher densities. Above the Ohmic divertor detachment threshold density,  $C_{Ar}$  and  $\eta_{Ar}$  both decrease as seen in Fig. 4 (solid squares). The number density of impurities in the core plasma increases as  $\overline{n_e^{core}}$  is increased past the detachment threshold and the number of neutral impurities measured in the divertor decreases. The argon enrichment value drops due to the fact that the

argon compression decreases after detachment, yet the deuterium compression remains constant (Fig. 4(b)). This decrease in both  $C_{Ar}$  and  $\eta_{Ar}$  is another disadvantage of detached divertor plasmas in comparison to plasmas in the high-recycling regime [18].

During enhanced-D $_{\alpha}$  (EDA) H-mode operation [19], impurity compression and enrichment ratios decrease from their L-mode values as seen in Fig. 4 (open circles). This change in  $C_{Ar}$  is due both to an increase in the core impurity ion density and a decrease in the divertor impurity neutral density. Because of the change in transport associated with EDA H-mode [15], the argon level in the core increases to a larger but steady-state value. The deuterium compression also decreases when the plasma goes into H-mode. The decrease in  $\eta_{Ar}$  observed is due to a larger decrease in  $C_{Ar}$  than in  $C_D$ .

Divertor detachment has been achieved with H-mode confinement on Alcator C-Mod [20]. Measurements of the argon compression and enrichment have been made for this type of discharge as well. They indicate that upon detachment of the divertor with H-mode confinement, the compression and enrichment values drop. These changes are not as dramatic as in an Ohmic or L-mode detachment and are not obvious from Fig. 4. (solid circles).

For similar Ohmic discharges, the compression and enrichment of the recycling impurities helium-3, neon, argon, and krypton have been compared. It is found that  $C_Z$  and  $\eta_Z$  both increase with impurity mass number. Such an increase in compression ratio between helium and neon is also observed on ASDEX-Upgrade [4]. It is also observed that the amount of degradation in compression after detachment depends on the mass of the impurity. Comparing measurements made at  $\bar{n}_e^{core} = 1.5 \times 10^{20} \text{ m}^{-3}$  (attached) to those made at  $\bar{n}_e^{core} = 2.8 \times 10^{20} \text{ m}^{-3}$  (detached) it is seen that there is a fractional change in argon compression of ~40% and in neon compression of ~15%. The deuterium compression actually increases between these values of line-averaged density.

#### 4. Discussion

The compression of impurities into the divertor depends on the balance of different forces along the magnetic field and on plasma flows as well as on ionization location and core transport [2,3]. At low density, the plasma flow in the Alcator C-Mod scrape-off layer is reversed near the separatrix and is toward the divertor farther out in the SOL. As the line-averaged density is increased to the detachment limit, the flow reversal weakens and the flow becomes toward the divertor across the whole SOL [21]. Thus the frictional force on impurities would act to increase compression during detachment. The temperature gradient along field lines increases only slightly after the divertor detaches. The combination of these forces does not change drastically during detachment. In addition, the core transport does not change measurably after detachment [8]. It can be postulated that the observed drop in argon compression after detachment is likely due to changes in the ionization location.

The ionization mean-free-path,  $\lambda_{\text{ion}}$ , can be written as:

$$\lambda_{\text{ion}} = \frac{v_{0,z}}{n_e \langle \sigma v \rangle_{\text{ion}}}, \quad (5)$$

where  $v_{0,z}$  is the velocity of the neutral impurity,  $n_e$  is the local electron density, and  $\langle \sigma v \rangle_{\text{ion}}$  is the cross-section for ionization. The cross-section for ionization is dependent upon the local electron temperature,  $T_e$ . Figure 5 is a plot of  $C_Z$  and  $\eta_Z$  versus ionization mean-free-path in a plasma with fixed  $n_e = 5 \times 10^{20} \text{ m}^{-3}$  and  $T_e = 10 \text{ eV}$  for the recycling impurities helium-3 (lower triangle), neon (upper triangle), argon (circle), and krypton (square). The neon, argon, and krypton measurements shown in Fig. 5 are from detached Ohmic plasmas. These conditions are typical of the plasma just beyond the detached region and the energy of the recycling impurity has been chosen to be a large fraction of the incident energy, in this case,  $2kT_e$ . The helium measurements were made in discharges with toroidal field of 7.9 T and an attached divertor because of the D-<sup>3</sup>He heating scheme used. It is seen that compression and enrichment are largest for impurities with the shortest ionization mean-free-path.

The ionization mean-free-path is important in the transition from attached to detached divertor, as indicated by the impurity mass dependence of compression degradation. In Ohmic detached plasmas, there is an extended region of plasma in the divertor with  $T_e < 1 \text{ eV}$  and  $n_e > 10^{21} \text{ m}^{-3}$  [22]. This region is clustered around the outer divertor leg and is within a few centimeters of the X-point. The  $\lambda_{\text{ion}}$  for such a plasma is much larger than the divertor dimensions for all impurities considered in this study. These impurities will readily traverse this region and should lead to easier penetration of the core plasma. This would result in the observed decrease of the impurity compression that occurs in Ohmic plasmas after detachment. The appearance of this region close to the separatrix also helps explain how the compression of argon is degraded by detachment more severely than neon or deuterium. Argon, which has a shorter  $\lambda_{\text{ion}}$  than neon or deuterium, no longer has an extended region of ionizing divertor plasma to screen it from the core. Therefore, impurities with short ionization mean-free-paths are affected most by detachment.

It has been reported previously [23] that the screening of argon improves, *i.e.* fewer argon atoms penetrate the core, as the density is raised below the detachment limit. This has been ascribed to the high density and large power flows in the SOL. It is also seen from Eq. (5) that for a given temperature in the divertor, an increase in the local density will result in a shorter  $\lambda_{\text{ion}}$ . This also would decrease the number of impurities penetrating the core and increase the compression.

## 5. Conclusions

Impurity transport has been investigated on Alcator C-Mod by measuring the impurity compression and enrichment factors for a variety of discharge conditions. Compression ratios of up to 400 and enrichment factors of up to twenty for puffed argon have been measured for

lower single-null divertor discharges. Compression ratios increase with increasing line-averaged density up to the detachment threshold due to the improved screening of impurities at higher density. Enrichment values remain constant or slightly increase with increasing line-averaged density up to the detachment threshold. This is because the compression of deuterium is increasing with line-averaged density almost as fast as the argon compression. Although the available data for other recycling impurities such as helium, neon, and krypton is sparse, these scalings appear to hold for these impurities as well.

Above the Ohmic divertor detachment threshold, the argon compression and enrichment fall precipitously. The compression ratio drops because the screening of impurities decreases when the divertor detaches. The enrichment value decreases because, in contrast to the argon compression dropping, the deuterium compression remains essentially constant after divertor detachment.

Measurement of impurity compression ratios and enrichment values have also been made in H-mode plasmas. It is found that compression and enrichment values are much smaller than their L-mode values. This is due mostly to an increase in the core impurity density from the enhanced confinement characteristic of the H-mode plasma. The divertor neutral impurity density decreases slightly, as does the divertor neutral deuterium density as the plasma enters the H-mode regime.

As is observed on other tokamaks, impurity compression and enrichment values increase with increasing atomic mass number. The ionization mean-free-path for impurities in the divertor plasma appears to be a crucial variable in describing the results. Different recycling impurities have different ionization mean-free-paths due to the different cross-sections and masses. As the ionization mean-free-path decreases, the impurity compression and enrichment values increase, that is, the easier it is for an impurity to be ionized, the easier it is to compress that impurity into the divertor. These experiments bode well for the ability to operate with an impurity-seeded radiative divertor that simultaneously retains a clean core plasma. This should be possible in a radiative, high-recycling divertor that is very nearly detached.

## **Acknowledgments**

This work is supported by U.S. Department of Energy Contract No. DE-AC02-78ET51013. The authors would like to thank G. McCracken, S. Krasheninnikov, and B. LaBombard for helpful discussions.

## **References**

- [1] G. Janeschitz, ITER-JCT, and Home Teams, *Plasma Phys. Controlled Fusion* **37** (1995) A19.
- [2] J. Neuhauser, W. Schneider, R. Wunderlich, and K. Lackner, *Nucl. Fusion* **24** (1984) 39.
- [3] P.C. Stangeby and J.D. Elder, *Nucl. Fusion* **35** (1995) 1391.

- [4] H.S. Bosch, D. Coster, R. Dux, *et al.*, J. Nucl. Mater. **241-243** (1997) 82.
- [5] M.J. Schaffer, M.R. Wade, R. Maingi, *et al.*, J. Nucl. Mater. **241-243** (1997) 585.
- [6] N. Richard, B. Terreault, E. Haddad, *et al.*, J. Nucl. Mater. **241-243** (1997) 760.
- [7] I.H. Hutchinson, R. Boivin, F. Bombarda, *et al.*, Phys. Plasmas **1** (1994) 1511.
- [8] G.M. McCracken, R.S. Granetz, B. Lipschultz, *et al.*, J. Nucl. Mater. **241-243** (1997) 777.
- [9] Prisma™ QMS200, product sold by Pfeiffer Vacuum Technology.
- [10] N. Hosogane, M. Shimada, K. Shimizu, *et al.*, J. Nucl. Mater. **220-222** (1995) 415.
- [11] J.F. O'Hanlon, *A User's Guide to Vacuum Technology*, John Wiley & Sons, New York (1989).
- [12] M. Brambilla, Max-Planck-Institut für Plasmaphysik, IPP Report 5/66 (1996).
- [13] M.A. Graf, J.E. Rice, J.L. Terry, E.S. Marmor, J.A. Goetz, G.M. McCracken, F. Bombarda, and M.J. May, Rev. Sci. Instrum. **66** (1995) 636.
- [14] R.A. Hulse, Nuclear Technology/Fusion **3** (1983) 259.
- [15] J.E. Rice, J.L. Terry, J.A. Goetz, *et al.*, Phys. Plasmas **4** (1997) 1605.
- [16] J.E. Rice and E.S. Marmor, Rev. Sci. Instrum. **61** (1990) 2753.
- [17] A. Niemczewski, I.H. Hutchinson, B. LaBombard, B. Lipschultz, and G.M. McCracken, Nuclear Fusion, **37** (1997) 151.
- [18] J.A. Goetz, C. Kurz, B. LaBombard, *et al.*, Phys. Plasmas **3** (1996) 1908.
- [19] Y. Takase, R.L. Boivin, F. Bombarda, *et al.*, Phys. Plasmas **4** (1997) 1647.
- [20] B. Lipschultz, J.A. Goetz, B. LaBombard, G.M. McCracken, H. Ohkawa, Y. Takase, J.L. Terry, J. Nucl. Mater. **241-243** (1997) 771.
- [21] B. LaBombard, J.A. Goetz, I.H. Hutchinson, *et al.*, in *Proceedings of the 16th International Atomic Energy Agency Fusion Energy Conference* (IAEA, Vienna, 1997), Vol 1, p. 825.
- [22] J.L. Terry, "On the experimental determination of the volume recombination rate in tokamak divertors", this conference.
- [23] G.M. McCracken, F. Bombarda, M.A. Graf, *et al.*, J. Nucl. Mater. **220-222** (1995) 264.



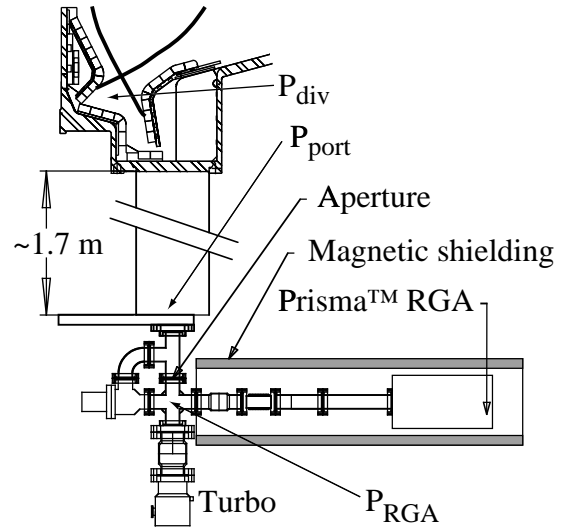


Fig. 1. Schematic showing the location of the RGA with respect to the lower closed divertor of Alcator C-Mod. The vertical port, the conductance-limiting aperture, and the RGA volume are shown as well as the pressure measurement locations.

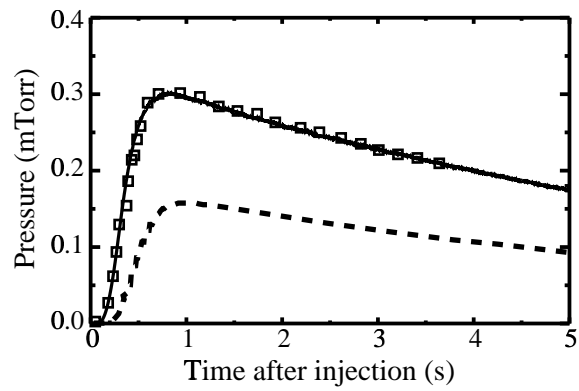


Fig. 2. An argon gas puff into an empty torus is used to determine RGA sensitivity. Shown are the pressure in the torus (solid line) measured with an ion gauge, the partial pressure ( $\times 2000$ ) in the RGA volume,  $P_{\text{RGA}}$  (dashed line), and the deconvolved torus pressure,  $P_{\text{div}}$  (squares). The RGA sensitivity for argon is  $3.5 \times 10^{-4}$  A/Torr.

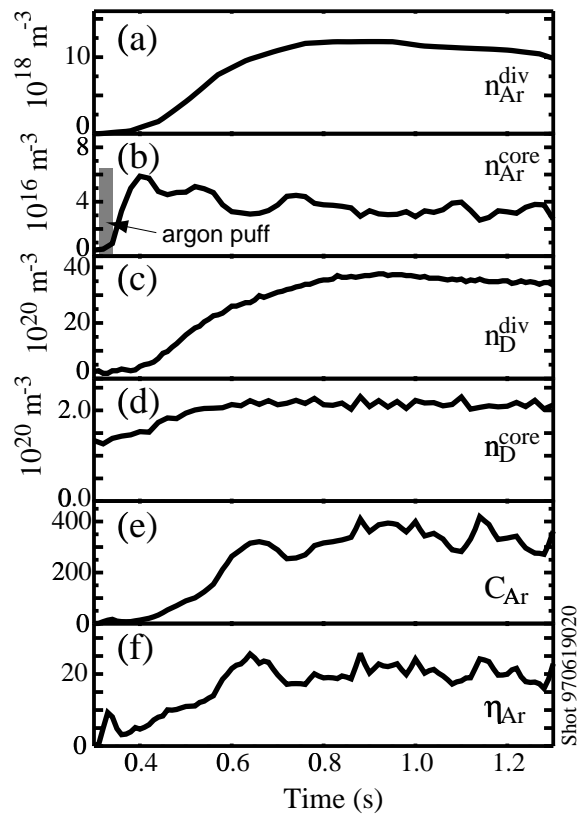


Fig. 3. Argon compression (e) and enrichment (f) values measured in a 1.0 MA Ohmic SN attached divertor discharge. Also shown are the argon and deuterium densities measured in the divertor and core plasmas.

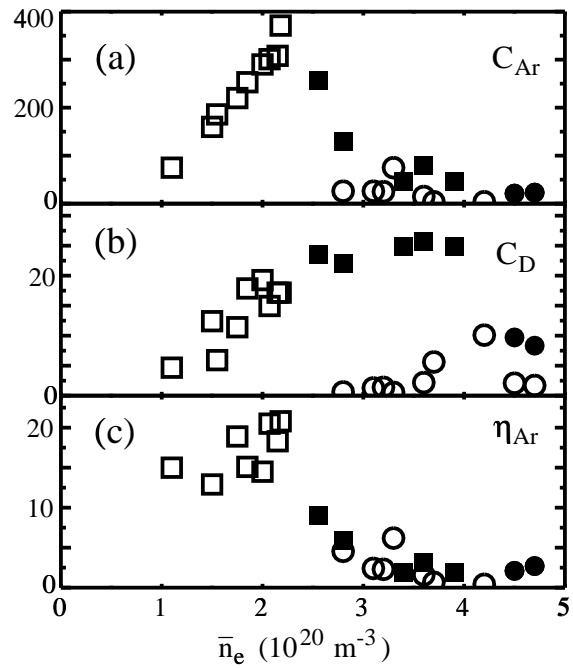


Fig. 4. Argon compression (a) and enrichment (c) values are measured in Ohmic (squares) and H-mode (circles) discharges. Detached divertor discharges are represented with filled symbols. Also shown are the measured deuterium compression values (b).

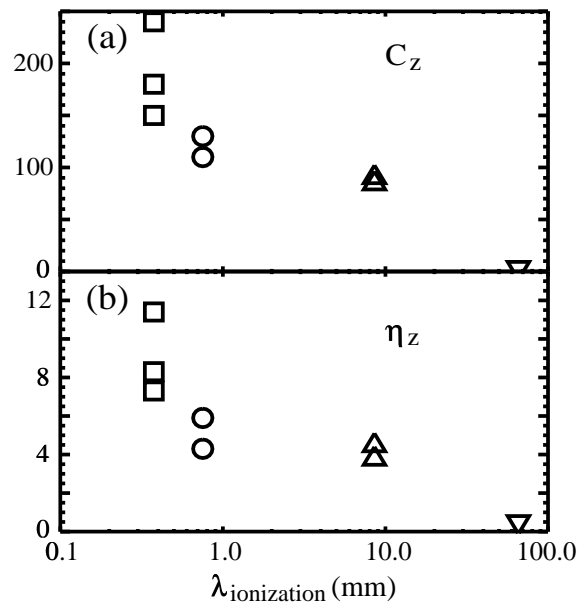


Fig. 5. Impurity compression (a) and enrichment (b) are dependent on the first ionization mean-free-path of the impurity. Shown are *detached* discharges with puffed krypton (square), argon (circle), neon (up triangle). The helium (down triangle) discharges are not detached. The  $\lambda_{\text{ionization}}$  is calculated for a 10 eV,  $5 \times 10^{20} \text{ m}^{-3}$  background plasma.